Study of the CMS RPC Efficiency during Run II Program of the LHC

Muhammad Abdullah Al-Mashad
(muhammad.muhammad@cern.ch)

Hemida Hamed Mohammed
(hemida.mohammed@cern.ch)

Supervised by: Dr. **Mohammed Attia Mahmoud**
(mohammed.attia@cern.ch)

21 June 2021 - 13 August 2021

Contents

List of Figures

Abstract

During RUN II of the LHC, the RPC system is running smoothly and collecting data for physics analysis. The performance of the system is closely monitored and studied. Here the results for the efficiency studies are shown. The RPC system is a very dynamic working system, which has a constantly changing working conditions during data taking periods. RPC efficiency studies allow for monitoring the system performance in a lot of different levels and quickly identifying and fixing any possible operational problems.

1 Resistive Plate Chambers

Resistive Plate Chambers (RPCs) are planar gaseous detectors, which have a very good time resolution, and also an adequate spatial resolution, simple design and low cost.

1.1 Detector Design

In the CMS detector the RPC system consists of 1056 double-gap chambers operating in avalanche mode [1]. Each RPC detector relies on two High Pressure Laminate (HPL) Bakelite gaps with 2 mm gas space between the plates [2] as shown in Figure 1. The HPL electrodes bulk resistivity is of the order of 1 – 6 x 10^{10} Ωcm. The plates in each gap are separated by a 10 x 10 cm^2 grid of plastic pieces called spacers in order to avoid contact due to the electrical attraction between them. The inside surface of the gaps is coated with a 35 to 45 µm linseed oil [3] in order to smoothen the surface and quench the Ultraviolet (UV) photons [4]. The outer surfaces of the gaps are coated with conductive graphite paint, thus forming the High Voltage and ground electrodes. The two gaps are placed one on top of another with a common readout performed by copper readout strips placed in between and isolated from the graphite by mylar sheets.

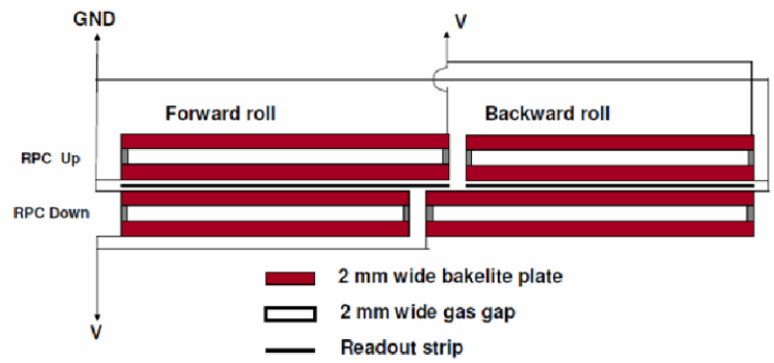

Figure 1: Schematic view of RPC double-gap design.

1.2 Detector Layout

In the CMS detector the need to trigger on the transverse momentum p_T of passing muons is the main purpose behind the detector layout of the RPC system. The p_T is measured with the bending of the muon in the CMS magnetic field and this requires a muon to cross at least 3 out of 4 layers in the Muon system. These layers are interleaved with the steel return yokes ensuring a maximum muon track bending between them.

The RPC system is divided into two regions following the CMS experiment configuration which are: Barrel region and Endcap region. It is composed of 1056 chambers covering a pseudorapidity range of $|\eta| < 1.2$ in the Barrel and $0.9 < |\eta| < 1.9$ in the Endcap. It has more than 110 000 electronic channels and covers a sensitive area of 3500 m^2 .

1.2.1 Barrel Region

The Barrel system consists of 480 RPCs, distributed equally among 5 wheels along the beam pipe (Wheel 0, Wheel ±1, Wheel ±2). As shown in Figure 2, each wheel consists of 4 stations (RB1, RB2, RB3 and RB4) with increasing radius R, which are interleaved with the steel return yoke. According to the direction of the azimuthal angle ϕ, each wheel is divided into 12 sectors (S01-S12), as dictated by the mechanical construction of the CMS return yoke. Due to mechanical reasons, RB3 and RB4 are further divided to + and − along ϕ in all sectors apart from S04, S09 and S11 in RB4. Since RB4/S09 and RB4/S11 are in the feet of the barrel wheel, they consist of only a single RPC chamber. RB4/S04 is divided even more along 4 chambers (++, +, −, − −).

Further to the trigger requirements, the chambers are divided with respect to pseudorapidity in 2 partitions, called rolls (forward and backward). Only RB2in in Wheels -1, 0, +1 and RB2out in Wheels -2, +2 are divided in 3 rolls (forward, middle and backward)[5].

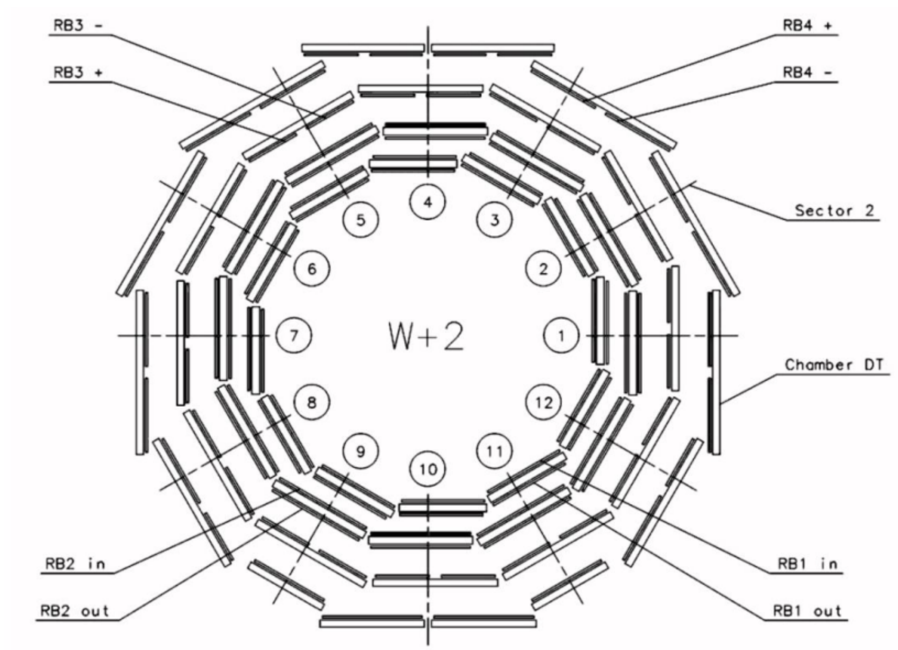

Figure 2: Sketch of one of the 5 Barrel wheels with its numbered sectors.

1.2.2 Endcap Region

The design in the Endcap is very similar to the one used in the Barrel. The main difference comes from the geometry aspects and the fine segmentation which higher multiplicity in the forward regions require.

The Endcap system consists of 576 RPCs, which are distributed along 8 disks named RE ± 1, RE ± 2, RE ± 3 and RE ± 4 [4 disks per each endcap (positive and negative)], as shown in Figure 3. The two disks for the fourth stations both positive and negative are instrumented with 144 RPC detectors during the Long Shutdown 1 (LS1) Muon system upgrade (2013-2014). Each disk is divided into 36 sectors along ϕ, and has two concentric rings [ring 2 (R2) and ring 3 (R3)]. There are 36 10° trapezoidal RPC chambers building up each ring, which are further divided into three rolls, labeled A, B and C with respect to increasing η. Each chamber is indicated as a segment CH01 through CH36 within a ring. Segment CH01 lays on the positive X-axis direction and the numbering proceeds anti-clockwise in respect to the interaction point.

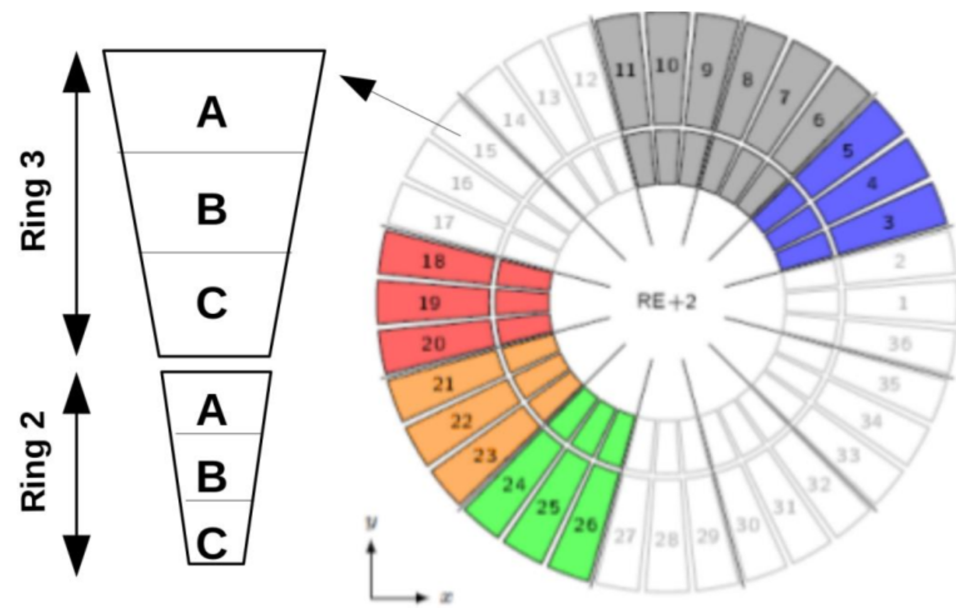

Figure 3: Sketch of one of the Endcap disks with its numbered sectors.

2 RPC Efficiency Studies

Efficiency of the RPC detector is calculated using the segment extrapolation method [6] which is the ratio between the number of detected and matched hits and the number of expected hits:

$$\eta_{RPC} = \frac{N_{detected}}{N_{expected}}.100\% \tag{1}$$

The amount of collected data has a great influence on the number of extrapolated segments. In case of large statistics, the efficiency estimation error is calculated by the equation:

$$\Delta\eta_{RPC} = \sqrt{\frac{(1-\eta_{RPC}).\eta_{RPC}}{N_{expected}}}.100\% \tag{2}$$

The chamber efficiency map for one wheel and one disk measured at a center-of-mass energy $\sqrt{s} = 13$ TeV is shown in Figure 4. Each part of the RPC system has a similar map, as they allow for quick and accurate detection of possible operational problems (gas leaks, noisy strips, etc).

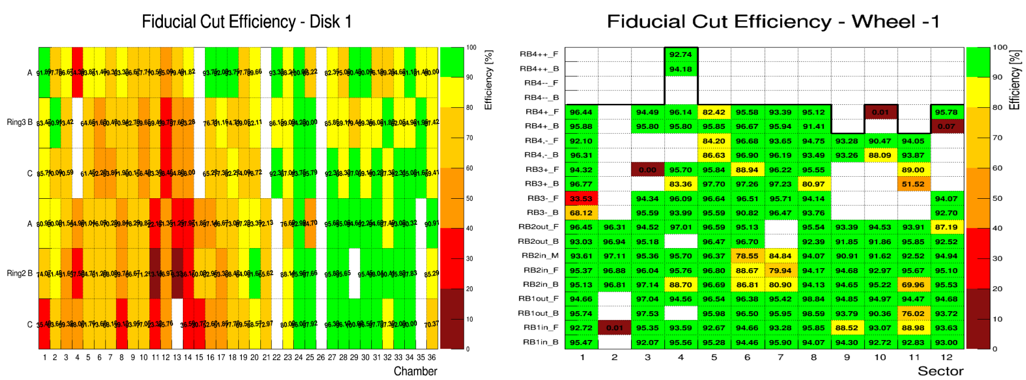

Figure 4: Chamber efficiency maps for Disk 1 (left), and Wheel-1 (right), from MWGR4 Run 342154 [7].

3 Results

The chamber efficiency maps for wheels and disks measured at a center-of-mass energy $\sqrt{s} = 13$ TeV from MWGR4 for Run 342154 [7] and Run 342156 [8] which we have worked on are shown in Figure 5 for wheels and Figure 6 for disks for Run 342154 and Figure 7 for wheels and Figure 8 for disks for Run 342156.

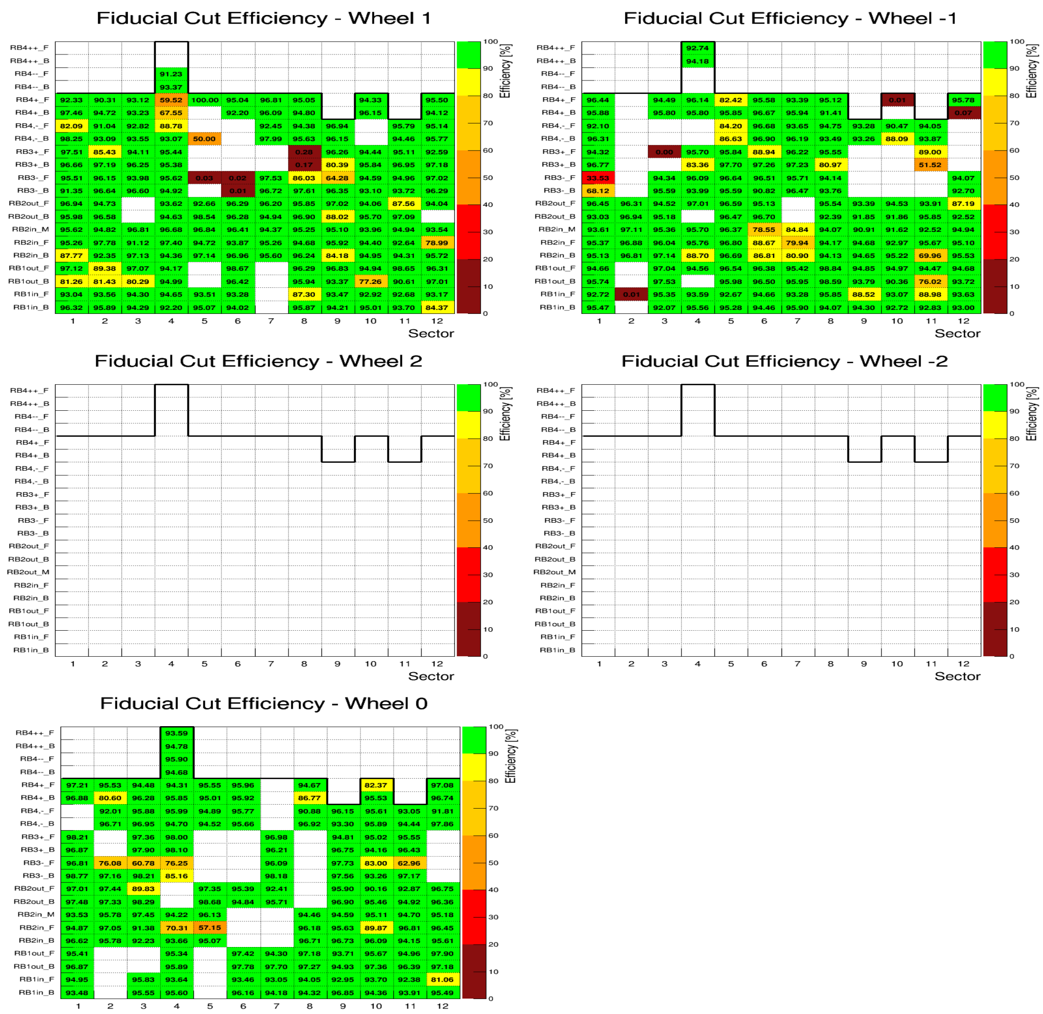

.

Figure 5: Chamber efficiency maps for Wheels, from MWGR4 Run 342154 [7].

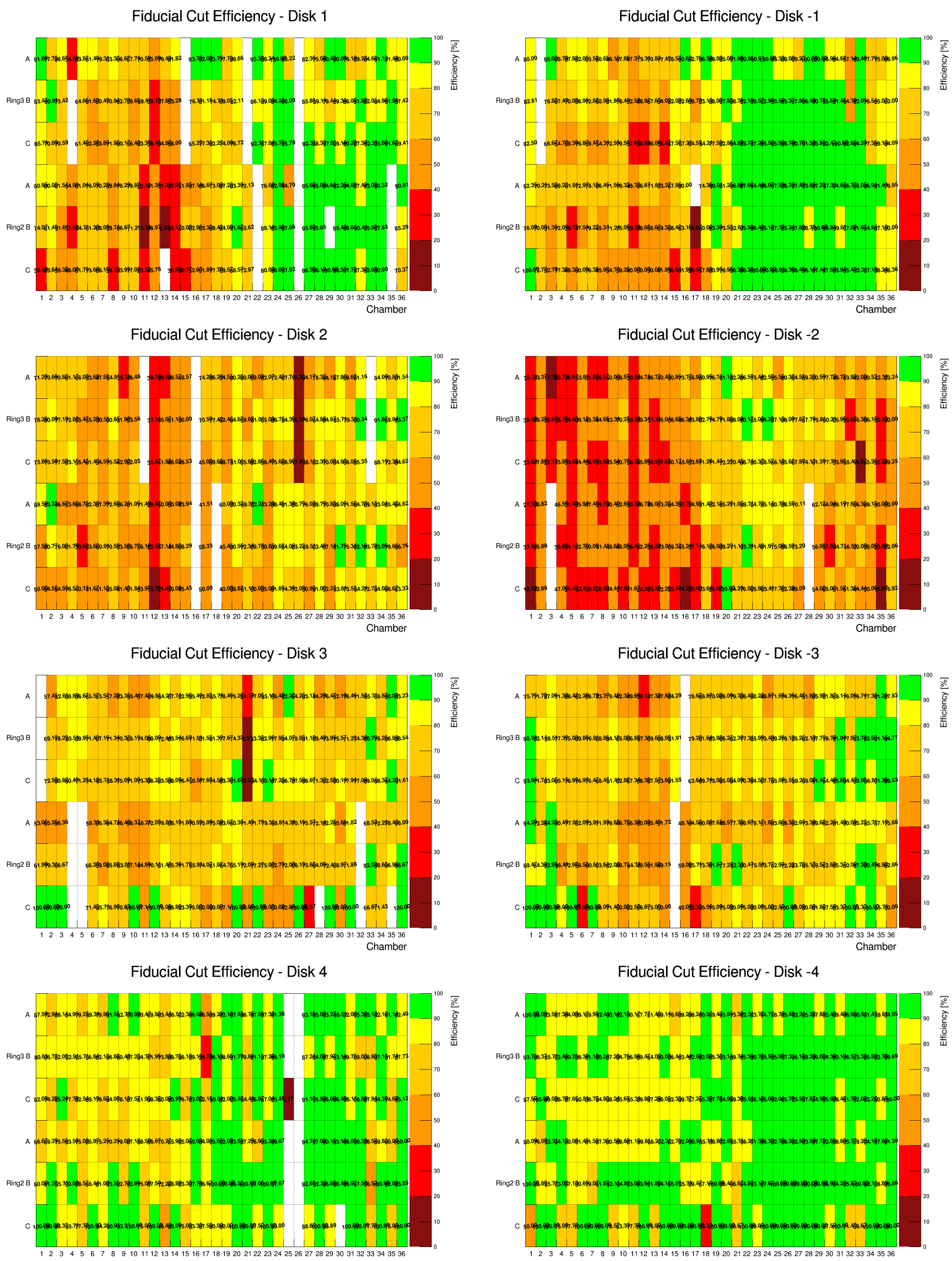

Figure 6: Chamber efficiency maps for Disks, from MWGR4 Run 342154 [7].

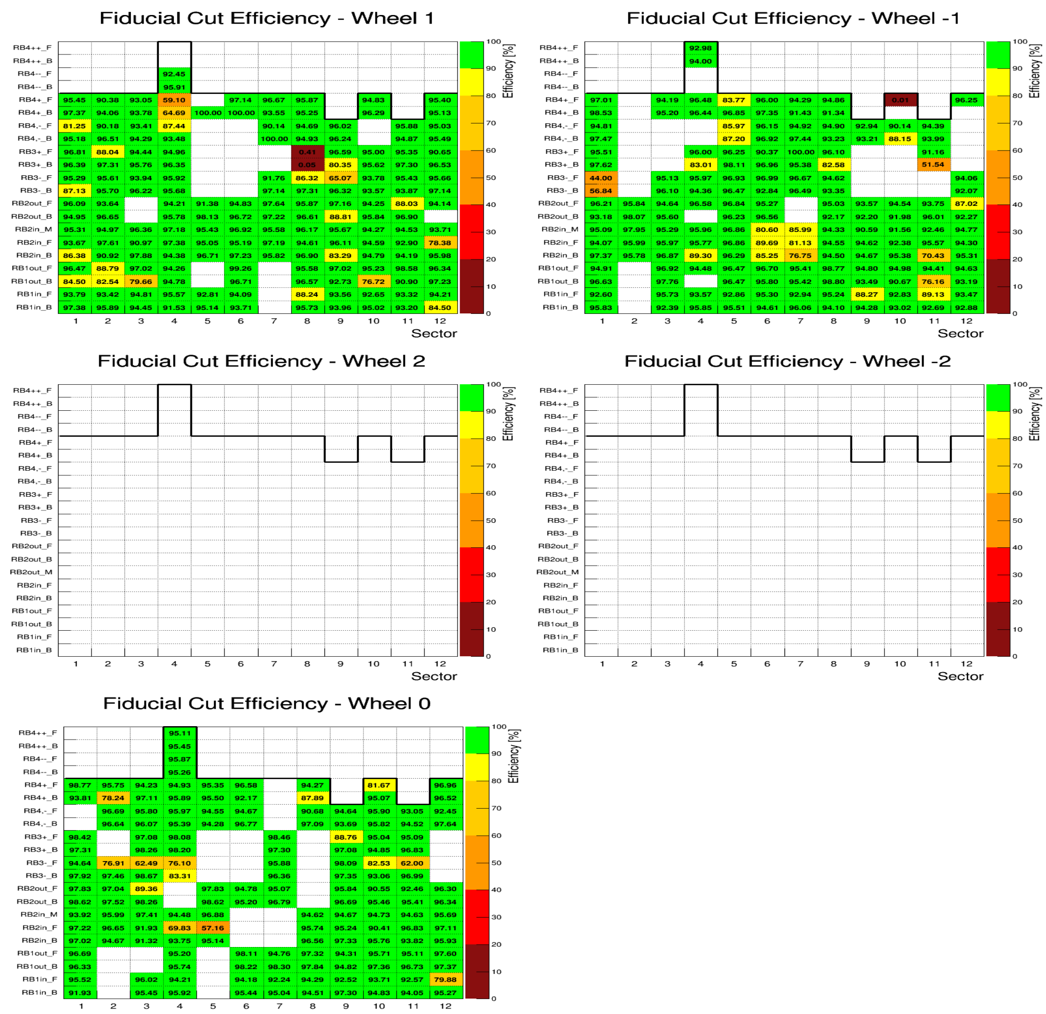

.

Figure 7: Chamber efficiency maps for Wheels, from MWGR4 Run 342156 [8].

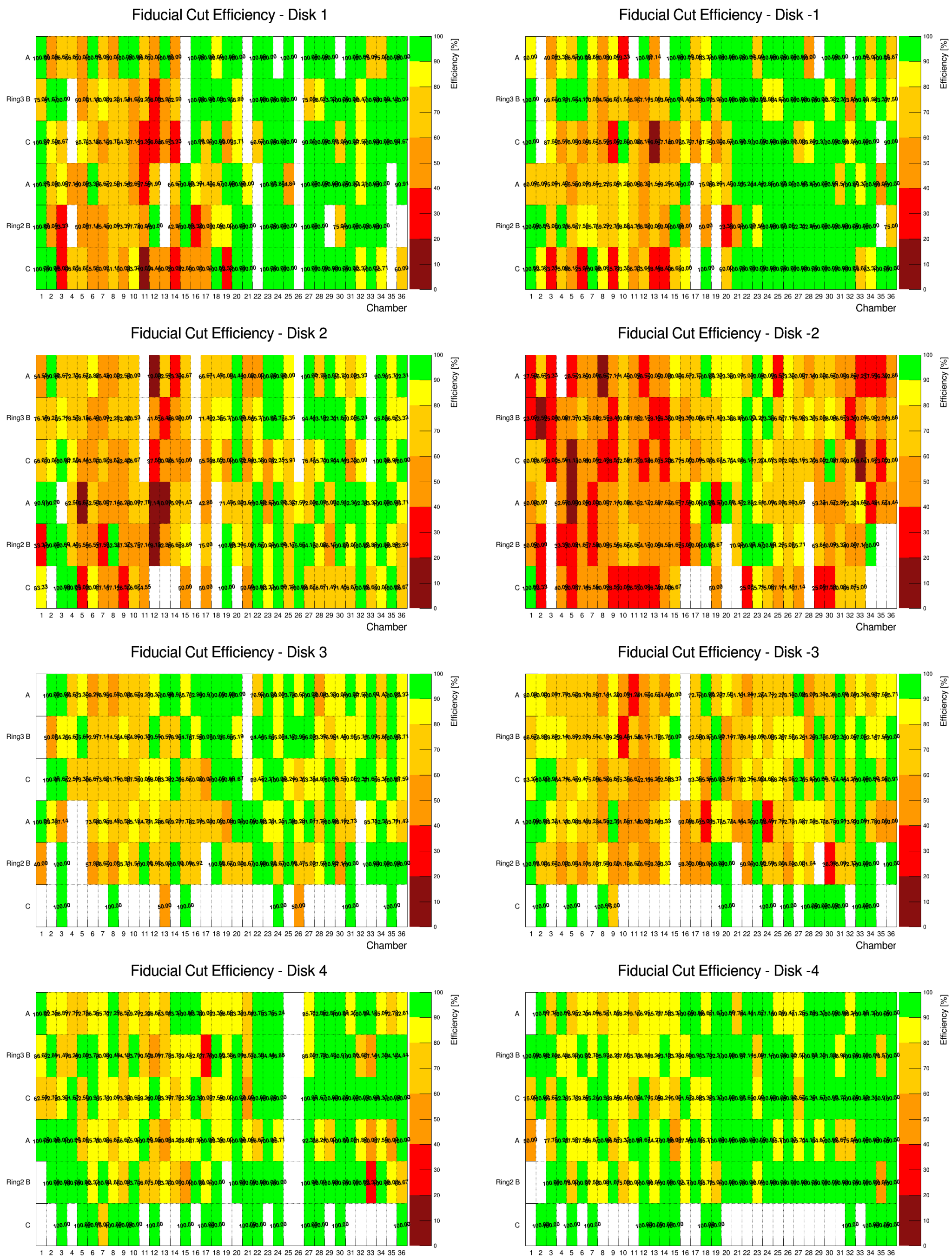

Figure 8: Chamber efficiency maps for Disks, from MWGR4 Run 342156 [8].

4 Conclusion

As shown from the results it is clear that there was a problem with Wheel+2 and Wheel-2 for the two Runs. In addition the empty chambers and low efficiency chambers need to be checked out for identification of the problems and fixing them. The RPC efficiency studies allow for quickly identifying and fixing any operational problems.

References

[1] CMS Collab. CMS Physics Technical Design Report. Vol. I: Detector Performance and Software, CERN/LHC, 1, 2006.

[2] Abbrescia M. et al. (2005) Cosmic ray test of double-gap resistive plate chambers for the CMS experiment, Nucl. Instr. Meth. A., 550, 116.

[3] M. Abbrescia et al., "Effect of the Linseed Oil Treatment on the Performance of the Resistive Plate Counters", Tech. Rep. CMS-NOTE-1997-018.

[4] L. Changguo, "RPC electrode material study", Nucl. Instrum. Meth. A , vol. 602, no. 3, pp. 761 – 765, 2009. doi:10.1016/j.nima.2008.12.225.

[5] CMS collaboration (1997) The Muon Project, CMS Technical Design Report, CERN/LHCC 97-32, CMS-TDR-003.

[6] C. Carrillo, Search for Heavy Stable Charged Particles in the CMS Experiment using the RPC Detectors, CMS-TS-2011-018, CERN-THESIS-2011-032.

[7] `https://cms-docs.web.cern.ch/cms-docs/MUON/dpgrpc/LS2/2021/mwgr4/342154/efficiency/`

[8] `https://cms-docs.web.cern.ch/cms-docs/MUON/dpgrpc/LS2/2021/mwgr4/342156/efficiency/`